Supplemental Figures and Legends

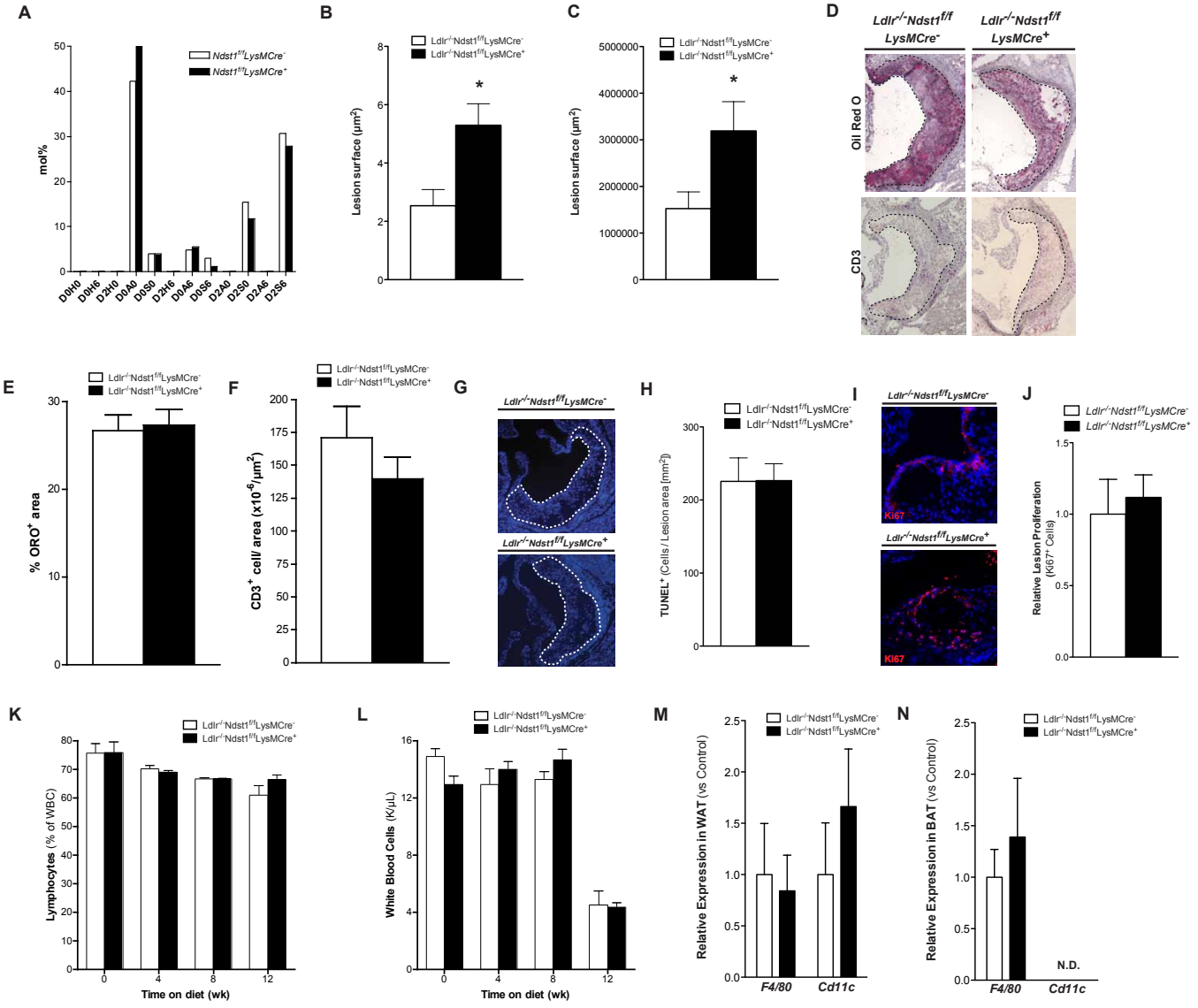

Supplemental Figure 1 – Related to Figure 2. (A) Changes in N-acetylated, N-sulfated, 2-O-sulfated and 6-O-sulfated HS disaccharide in Ndst1$^{f/f}$LysMCre^{+} BMDMs compared to wild-type BMDMs. (B-C) En face analysis of atherosclerosis and quantification of Sudan IV positive area in male *Ldlr$^{-/-}$Ndst1$^{f/f}$LysMCre^{-}* and *Ldlr$^{-/-}$Ndst1$^{f/f}$LysMCre^{+}* mice after 12 weeks on a HFC-diet (n = 3-5/group) (E and F). (D) Atherosclerotic lesions stained with Oil Red O or for T-Cells (CD3). (E) Quantification of Oil red O positive area in lesions from *Ldlr$^{-/-}$Ndst1$^{f/f}$* and *Ldlr$^{-/-}$Ndst1$^{f/f}$LysMCre^{+}* mice. (F) Quantification of CD3

positive cells per area in lesions from *Ldlr*$^{-/-}$*Ndst1*$^{f/f}$ and *Ldlr*$^{-/-}$*Ndst1*$^{f/f}$*LysMCre*$^{+}$ mice after 12-weeks HFC diet feeding. (G) Atherosclerotic lesions stained with TUNEL for apoptotic cells. (H) Quantification of TUNEL positive (red) nuclei (blue, Hoechst Dye) in lesions from *Ldlr*$^{-/-}$*Ndst1*$^{f/f}$*LysMCre*$^{-}$and *Ldlr*$^{-/-}$*Ndst1*$^{f/f}$*LysMCre*$^{+}$ mice. Atherosclerotic lesions stained for Ki67. (H) Quantification of Ki67 positive cells (red) nuclei (blue, Hoechst Dye) in lesions from *Ldlr*$^{-/-}$*Ndst1*$^{f/f}$*LysMCre*$^{-}$ and *Ldlr*$^{-/-}$*Ndst1*$^{f/f}$*LysMCre*$^{+}$ mice. (K) Evolution of the lymphocytes population in blood during HFC diet feeding. (L) Evolution of the white blood cell population in blood during HFC diet feeding. (M-N) Expression of F4/80 and CD11c in eWAT (M) and BAT (N) in *Ldlr*$^{-/-}$*Ndst1*$^{f/f}$*LysMCre*$^{-}$ and *Ldlr*$^{-/-}$*Ndst1*$^{f/f}$*LysMCre*$^{+}$ mice after 16-weeks on a HFC diet (n = 4/group). Shown are mean values ± SEM.

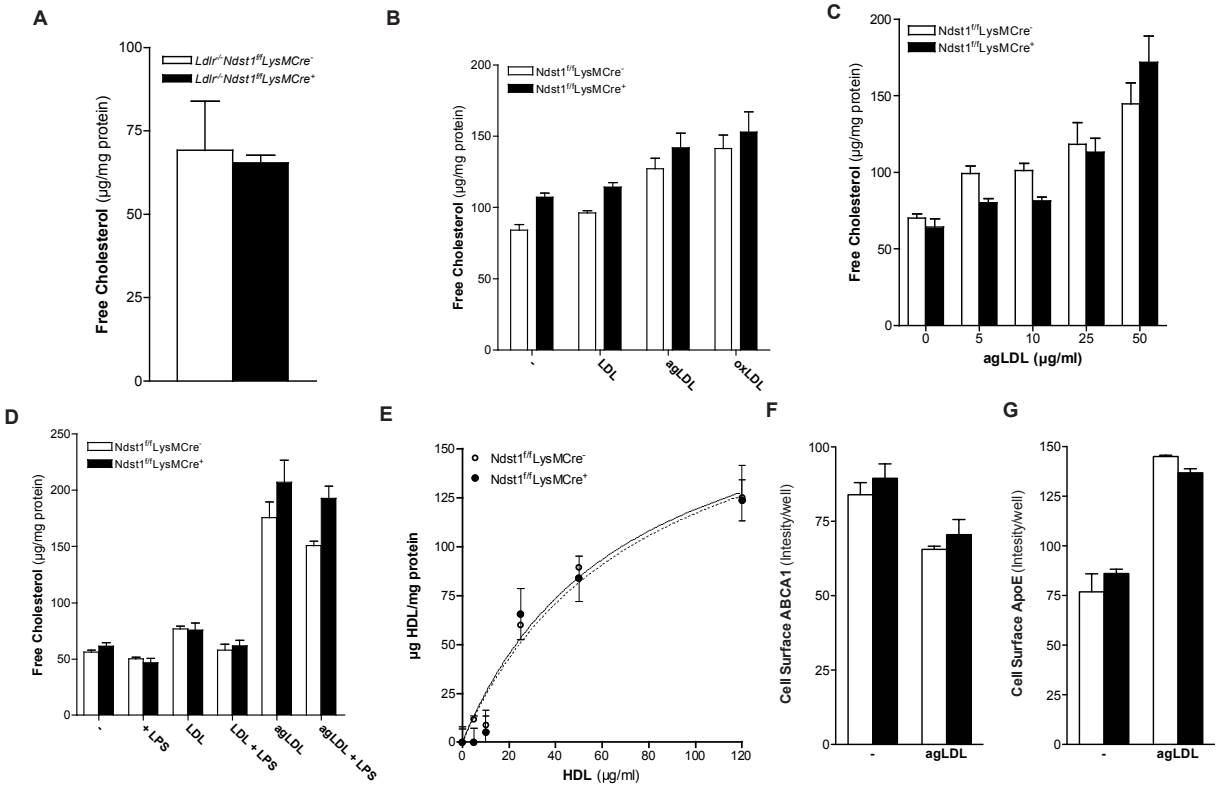

Supplemental Figure 2 - Related to Figure 3. (A) Quantification of free cholesterol levels in peritoneal macrophages collected after 12-weeks HFC diet feeding (n = 3 per group). (B) Quantification of free cholesterol levels in BMDM after a 24 hr incubation with 0 or 50 µg/ml of LDL, agLDL and oxLDL (n = 3). (C) Quantification of free cholesterol levels in BMDM after a 24 hr incubation with different concentrations of agLDL (n = 3). (D) Quantification of free cholesterol levels in BMDM after a 24 hr incubation with 0 or 50 µg/ml of LDL and agLDL in the presence or absence of 100 ng/ml LPS (n = 3). (E) Binding at 4ºC for 1 hr of DiD-HDL in BMDMs (n = 3). (F) Cell surface ABCA1 levels in BMDMs before and after incubation with 50 µg/ml of agLDL for 24 hr. (G) Cell surface ApoE levels in BMDMs before and after incubation with 50 µg/ml of agLDL for 24 hr. Shown are mean values ± SEM.

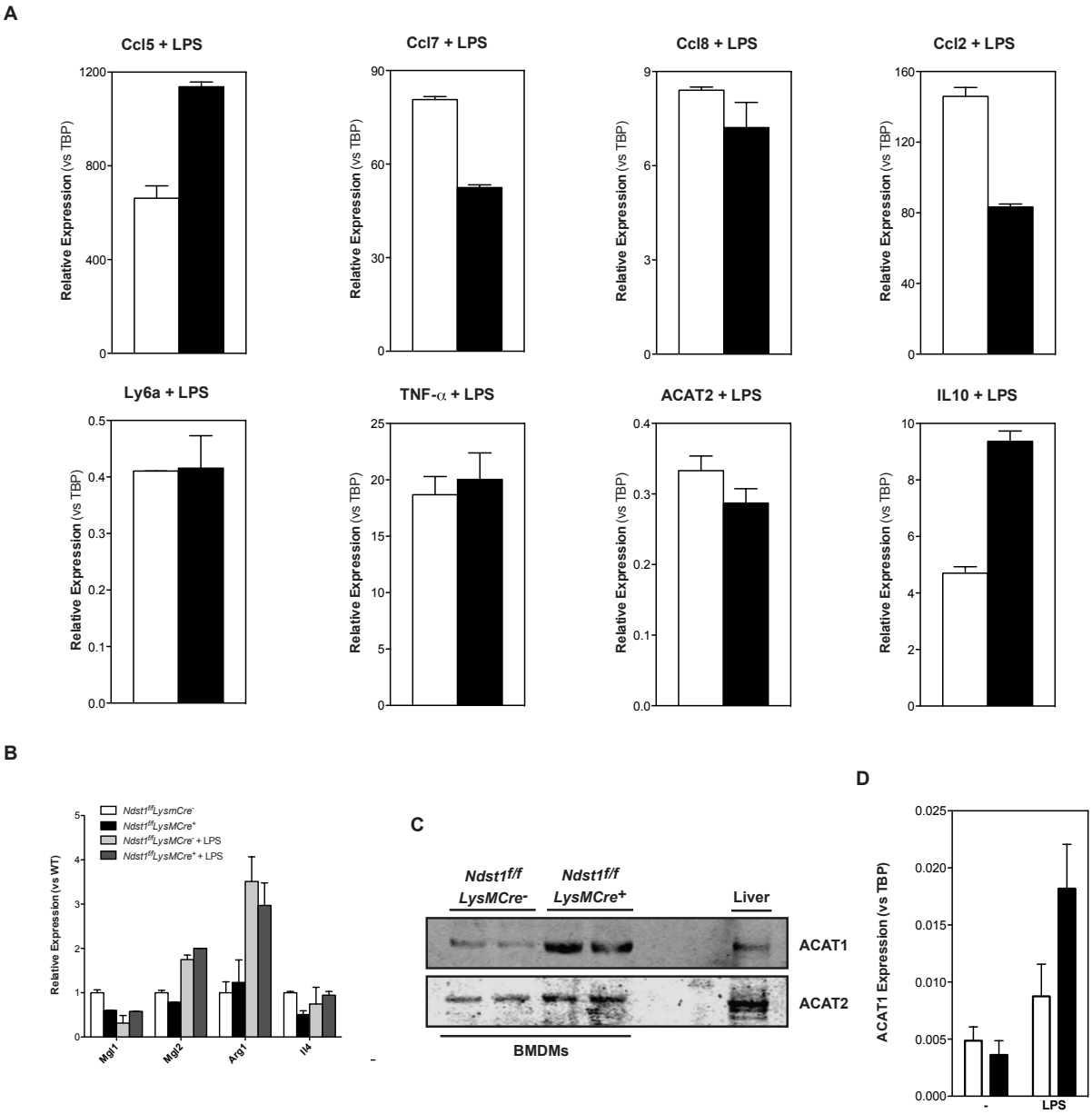

Supplemental Figure 3 - Related to Figure 4. (A) Real-time quantitative gene-expression validation of the indicated chemokines in wild-type and *Ndst1*$^{f/f}$*LysMCre*$^{+}$ BMDMs stimulated with 100 ng/ml LPS for 24 hr. (B) Expression of Mgl1, Mgl2, Arg1 and IL4 in wild-type and *Ndst1*$^{f/f}$*LysMCre*$^{+}$ BMDMs stimulated with or without 100 ng/ml LPS for 24 hr. (C) Immunoblot analysis of ACAT1, ACAT2 and β-actin in wild-type and *Ndst1*$^{f/f}$*LysMCre*$^{+}$ BMDMs. A wild-type liver homogenate was added as a positive control to validate the antibody specificities. (D) Expression of *Acat1* in wild-type and *Ndst1*$^{f/f}$*LysMCre*$^{+}$ BMDMs stimulated with or without 100 ng/ml LPS for 24 hr. Shown are mean values ± SEM.

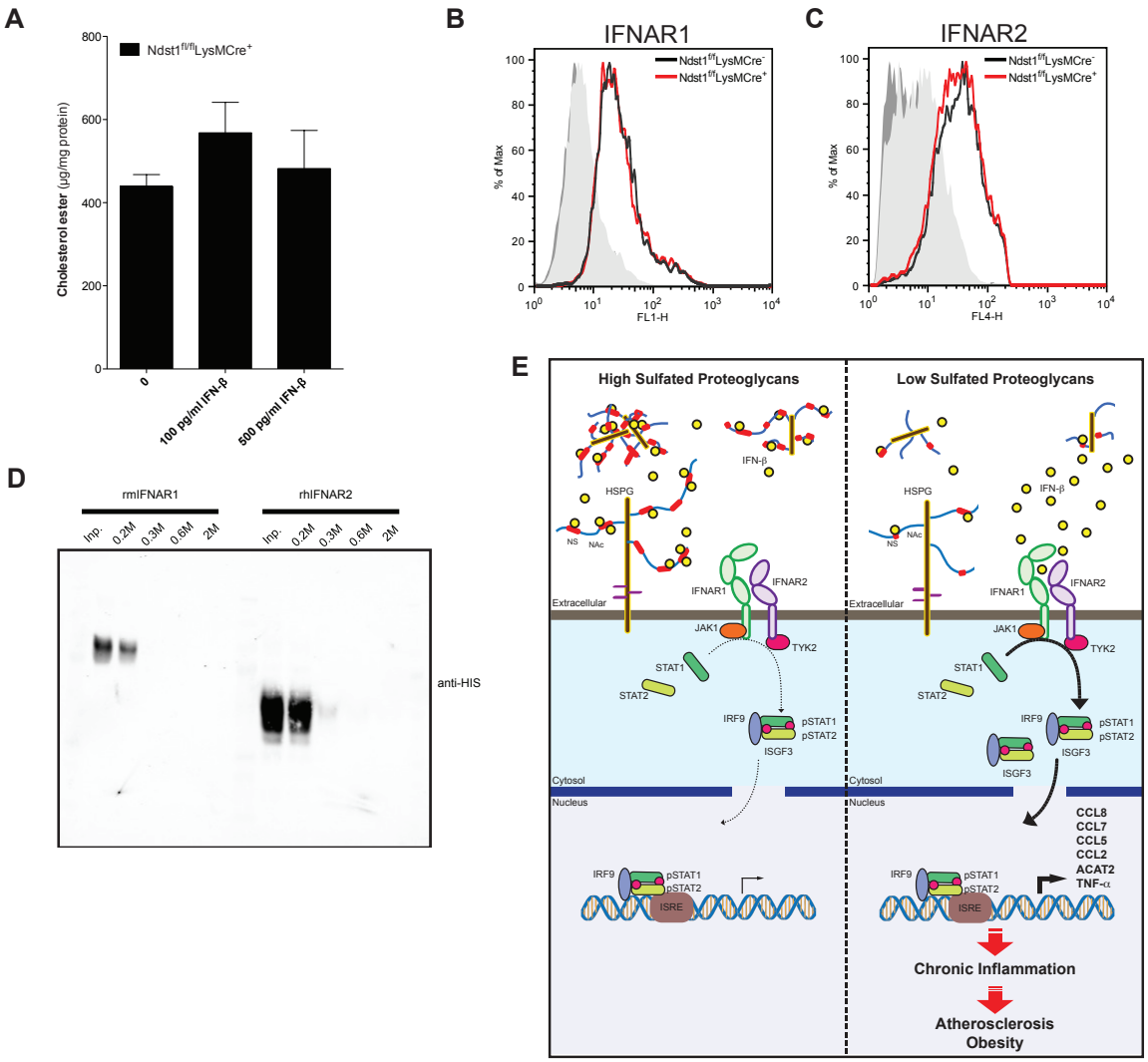

Supplemental Figure 4 - Related to Figure 7. (A) Cellular cholesterol ester levels were determined in *Ndst1*$^{f/f}$*LysMCre*$^{+}$ BMDMs stimulated with or without rmIFN-β for 24 hr after an additional 24 hr incubation with 100 µg/ml agLDL. (B-C) Cell surface expression of IFNAR1 (B) and IFNAR2 (C) as determined by flow cytometry. As a control, BMDMs were incubated with the respective secondary antibodies (filled gray histograms). (D) Expression of *Acat2* was evaluated in wild-type and *Ndst1*$^{f/f}$*LysMCre*$^{+}$ BMDMs incubated for 12 hr with an anti-IFNAR antibody or a control IgG (25 µg/ml). (E) Heparin-Sepharose chromatography of His-tagged recombinant mouse IFNAR1 (rmIFNAR1) and recombinant human IFNAR2 (rhIFNAR2) ectodomains. Western blotting was used to determine their input and elution from the column. No significant His-tag reactivity above 0.2 M NaCl was observed, which indicated no significant interaction of IFNAR1 and

IFNAR2 with heparin. (E) Proposed Model: HSPGs determine the bioavailability of IFN-β for its receptors IFNAR1 and IFNAR2 on macrophages. In resting conditions the highly sulfated HS produced by macrophages (left panel) maintain cells in a quiescent state through sequestration of low levels of IFN-β. Genetic or enzymatic reduction of cell-associated HSPGs (right panel) increases the bioavailability of IFN-β resulting in activation of macrophages by driving transcription of inflammatory genes. This shift in tonic Type I IFN signaling boosts the activation state of macrophages and sensitizes individuals to chronic inflammation that worsens metabolic diseases such as atherosclerosis and obesity. Shown are mean values ± SEM.

Supplemental Tables

Supplemental Table S1. See attached Excel file.

Supplemental Table S2. qPCR Primers

Gene	Forward primer (5'-3')	Reverse primer (5'-3')
ACAT1	GGACACATACAGAAATGGTCACAT	GCACAAAACCTAGAACTCCAAGTT
ACAT2	GACTTGGTGCAATGGACTCG	GGTCTTGCTTGTAGAATCTGG
CCL5	CAT ATG GCT CGG ACA CCA	ACA CAC TTG GCG GTT CCT
CCL7	CCTGGGAAGCTGTTATCTTCAA	TGGAGTTGGGGTTTTCATGTC
CCL8	GCTGTGGTTTTCCAGACCAA	GAAGGTTCAAGGCTGCAGAA
CD11c	ACACAGTGTGCTCCAGTATGA	GCCCAGGGATATGTTCACAGC
F4/80	CTTTGGCTATGGGCTTCCAGTC	GCAAGGAGGACAGAGTTTATCGTG
IL-10	TGAATTCCCTGGGTGAGAAG	TCACTCTTCACCTGCTCCACT
IL-1b	AAATACCTGTGGCCTTGGGC	CTTGGGATCCACACTCTCCAG
IL-6	CCAGAGATACAAAGAAATGATGG	ACTCCAGAAGACCAGAGGAAAT
Ly6A	ATGGACACTTCTCACACTACAAAG	TCAGAGCAAGGTCTGCAGGAGGACTG
MCP-1	AGGTCCCTGTCATGCTTCTG	GCTGCTGGTGATCCTCTTGT
TBP	GAAGCTGCGGTACAATTCCAG	CCCCTTGTACCCTTCACCAAT
TNFα	CCAGACCCTCACACTCAGATC	CACTTGGTGGTTTGCTACGAC
Arg1	ATGGAAGAGACCTTCAGCTAC	GCTGTCTTCCCAAGAGTTGGG
Clec10a (Mgl1)	ATGATGTCTGCCAGAGAACC	ATCACAGATTTCAGCAACCTTA
Mgl2	CAGAACTTGGAGCGGGAAGAG	TTCTTGTCACCATTTCTCATCTCCT
IL4	ATGGAGCTGCAGAGACTCTT	AAAGCATGGTGGCTCAGTAC

Supplemental Experimental Procedures

Mice

Ndst1$^{f/f}$*LysMCre*$^{+}$ mice were generated by crossing *Ndst1*$^{f/f}$ mice to *LysMCre* transgenic mice (Clausen et al., 1999). *Ldlr*$^{-/-}$ mice were purchased from The Jackson Laboratory and crossed with *Ndst1*$^{f/f}$*LysMCre*$^{+}$ mice to generate *Ldlr*$^{-/-}$*Ndst1*$^{f/f}$*LysMCre*$^{+}$ mice. All animals were fully backcrossed on C57Bl/6 background. All animals were housed and bred in vivaria approved by the Association for Assessment and Accreditation of Laboratory Animal Care located in the School of Medicine, UCSD, following standards and procedures approved by the UCSD Institutional Animal Care and Use Committee. Mice were weaned at 3 weeks, maintained on a 12-hour light cycle, and fed *ad libitum* with water and standard rodent chow (Harlan Teklad) or a high fat/high cholesterol diet (TD.88137 from Harlan Teklad, 0.2% cholesterol, 21% milk fat).

Cell culture

Macrophages were isolated from 8 to 14-week old female mice. Peritoneal macrophages were harvested by peritoneal lavage 4 days after i.p. injection of 3 ml of thioglycollate (BD Biosciences). Cells were cultured overnight and adherent macrophages were collected. BMDM were generated as described. The cells were cultured in DMEM/F12 (Life Science Technologies) containing 10% FBS, 100 units/ml penicillin, 100 µg/ml streptomycin and 20 ng/ml macrophage colony-stimulating factor (M-CSF) (Shenandoah Biotechnology, Inc.). Macrophages were obtained as a homogeneous population of adherent cells after 6 days of culture. Conditioned medium (24 hr) from BDMD was flash frozen and CCL5 and CCL7 secretion was determined using ELISA (eBioscience).

Heparan sulfate purification and disaccharide analysis

Bone marrow derived macrophages were treated with a trypsin (0.5% trypsin, 0.53 mM EDTA. MediaTech) for 10 min at 37ºC to release cell surface proteoglycans. The cells were pelleted and the trypsin supernatant was treated overnight with Pronase (2 mg/mL; Roche Diagnostics) to degrade proteins, followed by purification of the glycopeptides by anion exchange chromatography using DEAE-Sephacel (Amersham Biosciences). Columns were washed with low-salt buffer (0.15 M NaCl, 20mM sodium acetate; pH 6.0) to retain low-sulfated chains and then eluted with 1 M NaCl. Samples were desalted by gel filtration (PD-10 columns, GE Health Care) and then lyophilized. Chains were digested with recombinant heparin lyases I, II, and III. The resulting disaccharides were subsequently derivatized with isotopically labeled aniline and quantified by mass spectrometry as described previously (Lawrence et al., 2008). Molar percentages were calculated based on the relative area under each peak.

FGF2 Binding and protein expression analysis

BMDMs were grown to confluence in non-tissue culture treated petri dishes, lifted with 5 mM EDTA and washed once with PBS (Life Science Technologies). Cells were incubated with or without 5 mU/mL heparin lyase III in PBS with Ca^{2+} (Life Science Technologies) at 37ºC for 15 min and then with biotinylated FGF2 (bFGF2, Shenandoah Biotechnology). Cells were washed, and bound biotinylated FGF2 was detected using streptavidin-PE-Cy5 (1:1000, PharMingen) and flow cytometry (FacsCalibur, BD Biosciences). In other experiments, cells were incubated with antibodies against ABCA1

(Abcam, ab7360), ApoE (Meridian, K23100R), IFNAR1 (Millipore, 04-151) or IFNAR2 (R&D Systems, MAB1083) (1:100 dilution) for 30 min on ice. Bound antibodies were detected using DyLight 488-conjugated goat anti-rabbit IgG or DyLight 647-conjugated goat anti-mouse IgG (1:1000; Life Science Technologies). Data were analyzed by using FlowJo Analytical Software (Tree Star Inc.).

Plasma lipids and lipoprotein distribution and blood cell analysis

Blood was obtained by cardiac puncture from mice fasted for 16 hrs, or via tail the vein using microvette CB 300 capillaries (Sarstedt, Nümbrecht Germany) from mice fasted for 5 hrs. Plasma cholesterol and triglyceride levels (Sekesui, San Diego, CA, US) and NEFA levels (WAKO Diagnostics, VA, US) were measured by commercially available enzymatic kits (Tsimikas et al., 2011). Lipoprotein profiles were performed on pooled plasma from six mice per genotype. Lipoproteins in 200 µl pooled plasma samples were separated by fast performance liquid chromatography (FPLC) gel filtration on a Superose 6 column and cholesterol and triglycerides were determined in each fraction. Whole EDTA blood samples were analyzed in duplicate for CBC with leukocyte differential and platelets were counted on a Hemavet 850FS Multi Species Hematology System (Drew Scientific, CT) programmed with mouse hematology settings.

Quantification of aortic atherosclerosis

Female mice euthanized by CO_2 intoxication were perfused with 10 ml PBS. The heart and ascending aorta down to the iliac bifurcation were removed and incubated in paraformaldehyde (PFA, 4% [wt/vol] in PBS). The heart and adventitial tissue were

removed, the aortas were cut open along the long axis, pinned flat and stained for neutral lipids using Sudan IV. Images were acquired and lesions from blinded samples were measured using image J software (Tsimikas et al., 2011). In addition, aortic root cross-sectional atherosclerosis was measured by cutting 10 μm paraffin sections starting at the first leaflet of the aortic valve plane and proceeding distally for 1000 μm in 100-μm intervals and photomicrographs were taken with a 4X objective (Nikon eclipse 80i microscope). Modified van Gieson collagen staining was used to enhance the contrast between the intima and surrounding tissue. Lesion size was determined using ImageJ software and average values from multiple mice were determined by an investigator at the UCSD Metabolic and Molecular Physiology CORE blinded to the study.

Monocyte labeling in vivo.

Classical Ly-6Clo monocytes were labeled in vivo by retro-orbital i.v. injection of 1 μm Fluoresbrite green fluorescent (YG) plain microspheres (Polysciences Inc.) diluted 1:4 in sterile PBS 3 days after i.v. injection of 250 μl clodronate-loaded liposomes (Encapsula NanoSciences). Bead infiltration was analyzed as described (Tacke et al., 2007; Tacke et al., 2006).

Immunohistochemistry

Mice euthanized by isoflurane intoxication were perfused with PBS and 10% formalin (Fisher, SF93-4). The upper part of the hearts were placed onto a tissue mold, covered in OCT (Tissue-Tek), and frozen. Serial 10-μm cryosections from similar parts of the aortic sinus were used for staining with Oil Red O or for monocyte infiltration

experiments. All other tissues were embedded in paraffin, stained with hematoxylin and eosin or with rabbit antiserum against F4/80 (AbD Serotec, MCA4978) at a 1:50 dilution, anti-CD68 mAb (Biolegend, 137001) at a 1:100 dilution, anti-Caveolin (BD Bioscience, BDB610059) at a dilution of 1:100 or CD3 (AbD Serotec, MCA500G) at a 1:200 dilution. Rabbit IgG (Dako, K5207) was used as a negative control. Sections stained for CD3 were incubated with biotinylated goat anti-rabbit antibodies (Jackson ImmunoResearch Laboratories, 111-065-045) at a dilution of 1:100 and biotinylated goat anti-rat (BD Biosciences, 559286) at a dilution of 1:100. Horseradish peroxidase-conjugated streptavidin (016-030-084) at 1:500 dilution was used for sections stained with F4/80 and CD3. Alexa 488-streptavidin (Life Science Technologies, S11223) at a dilution of 1:400 or Cy3-streptavidin antibodies used for immunofluorescence (Jackson ImmunoResearch Laboratories Inc., 016160-084) at a dilution of 1:500. Sections were counterstained with Mayer's hematoxylin (Sigma-Aldrich) or Hoechst (Molecular Probes, 33258). TUNEL staining was carried out using the TMR red kit (Roche 12156792910). The contrast of all images was adjusted equally, and the extent of staining was measured with ImageJ software. Stained lesion areas in sections (n= 27-33 lesions) were quantitated using ImageJ software. The data was averaged and expressed as a percentage of the size of the lesion.

RNA analysis

Total RNA was isolated from homogenized tissue and cells in Trizol and purified using RNeasy columns and RNase free DNase digestion according to the manufacturer’s instructions (QIAGEN). The quality of the total RNA was monitored by the Agilent 2100 Bioanalyzer (Agilent Technologies, Palo Alto, CA) and RNA quantity was measured with

a NanoDrop (NanoDrop Technologies, Inc. Wilmington, DE) following the manufacturer's instructions. For quantitative PCR analysis, 1 µl of cDNA was used for real-time PCR with gene-specific primers (primer sequences indicated in Supplemental Table S2). Quantitative-PCR (SYBR Green) analysis was performed on an Applied Biosystems 7300 Real-time PCR system (Invitrogen). Global gene expression was measured by microarray analysis on RNA samples from two mice per strain for each treatment (basal medium and agLDL). The Affymetrix HT_MG430A array was used and the data was filtered as described (Bennett et al., 2010). Data are uploaded to the Gene Expression Omnibus (GEO) and readers can access the private data via the following link: http://www.ncbi.nlm.nih.gov/geo/query/acc.cgi?token=sxkbymogflovlsn&acc=GSE51009. Gene ontology (GO) analysis of microarray data was performed using the web-based DAVID Functional Annotation tool (http://david.abcc.ncifcrf.gov/home.jsp) (Huang da et al., 2009a; Huang da et al., 2009b). GO terms were considered significant if they had a Benjamini-corrected p value less than 0.05.

Lipoprotein binding and uptake

Human LDL (density δ 1.019-1.063 g/mL) and HDL (density δ 1.063-1.21 g/mL) was isolated from plasma by buoyant density ultracentrifugation as described (Deng et al., 2012) and quantified by BCA protein assay (Pierce). LDL was aggregated by gentle vortexing for 30 seconds as described (Khoo et al., 1992). To label the particles, agLDL (2 mg) was combined with 100 µL of 3 mg/mL 1,1‘-dioctadecyl-3,3,3’,3‘-tetramethylindodicarbocyanine perchlorate (DiD; Invitrogen) in dimethylsufoxide and then reisolated by ultracentrifugation. After incubation with agLDL, cells were rinsed with phosphate-buffered saline and lysed by adding 0.1 M sodium hydroxide plus 0.1%

sodium dodecyl sulfate for 40 min at room temperature (Deng et al., 2012). Fluorescence intensity was measured with appropriate excitation and emission filters in a plate reader (TECAN GENios Pro; Tecan, Switzerland) and normalized to total cell protein.

Foam cell assay and reverse cholesterol transport

Macrophage cholesterol ester content was quantitated by the Amplex Red Cholesterol Assay Kit (Life Science Technologies, San Diego). Macrophages were fixed in 2% paraformaldehyde for 2 min, washed three times with PBS, and incubated with 200 µl of absolute ethanol for 15 min at 4°C to extract cellular lipids. Cholesterol ester content was calculated by subtracting free cholesterol from total cholesterol for each sample. Lipid-extracted cells were scraped in 0.1% sodium dodecyl sulfate/0.1 M sodium hydroxide and after 30 min at 4ºC total cell protein was determined by the BCA protein assay. Cholesterol ester levels under different treatments were normalized to total cellular protein content.

Cholesterol efflux from BMDMs was performed according to established methods (Nakaya et al., 2011). BMDMs were labeled with [^{3}H]cholesterol (1 µCi/mL) and loaded with 50 µg/mL agLDL for 24 hrs. The cells were washed and equilibrated overnight in DMEM/F12 with 0.2% BSA. For cholesterol efflux, the medium contained 10 µg/mL human apoA-I or 50 µg/mL human HDL. After 24 hrs, an aliquot of the medium was removed, and the [^{3}H]cholesterol released was measured by liquid scintillation counting. The [^{3}H]cholesterol present in the cells was determined by extracting the cell lipids in absolute ethanol. The percentage cholesterol efflux was calculated by dividing the media-derived radioactivity by the sum of the radioactivity in the media and the cells.

Western blotting

BMDM were washed twice with PBS and treated with indicated concentrations of IFN-β in serum-free growth medium for 30 min at 37ºC. Selected samples were pretreated for 15 min with 5 mU/ml heparin lyase III at 37ºC. Cells were lysed and resolved by SDS-PAGE and blotted with antibodies to Stat1, phospho-STAT1 (Cell Signaling), ACAT1, ACAT2 (Santa Cruz Biotechnology) and β-actin (Sigma-Aldrich). Bands were visualized on an Odyssey Infrared imaging system (Li-Cor Biosciences) as described (Gonzales et al., 2013).

Indirect Calorimetry

Mice were placed into Comprehensive Lab Animal Monitoring System (CLAMS; Columbus Instruments) metabolic cages to adapt to their surroundings for 48 hours before study. Rates of O2 consumption (VO2; ml/kg/h) and CO2 production (VCO2) were measured for each chamber every 17 minutes throughout the study. EE was calculated as VO2 × (3.815 + [1.232 × (VCO2/VO2)]).

Glucose tolerance (GTT) and insulin tolerance test (ITT)

Mice were fasted for 5 hours. Blood samples were collected via tail vein bleeding immediately before and at 15, 30, 60, 90 and 120 min after oral glucose (2 mg/g body weight) gavage for GTT, after intraperitoneal injection of insulin (0.5U/g body weight) for ITT. Blood was immediately used for determination of the glucose levels via the Accu-

Chek® Aviva glucose monitoring system (Roche Applied Science GmbH, Mannheim, Germany). Insulin levels were determined via the ultra sensitive rat insulin ELISA kit (Chrystal Chem, Downers Grove, IL) as described by the manufacturer's instructions.

Nitrocellulose filter binding assay

Recombinant IFNAR1 (Life Science Technologies), IFNAR2, IFN-α4 and IFN-β (400 or 800 ng; PBL Interferon) were incubated with 10,000 counts of ^{35}S-labeled BMDM HS in 100 µL of PBS for 1 hr at 22 °C. The mixtures were applied to a prewashed nitrocellulose membrane in a Bio-Rad 96-well blot apparatus and washed with 100 µL of PBS twice. Free [^{35}S]HS passed through the membrane, and only the portions that bound to protein were retained as described (Maccarana and Lindahl, 1993). Bound material was eluted with 0.5 mL of HEPES buffer containing 2 M NaCl. Released [^{35}S]HS was measured by liquid scintillation counting. The extent of binding was quantified by dividing the counts retained by the membrane by the total input counts.

Recombinant IFNAR1, IFNAR2 and IFN-β (200 µg) were applied to a 1-mL HiTrap heparin-Sepharose column (GE Healthcare) and eluted with sequential increasing salt concentrations (150 mM, 300mM, 600mM and 2 M NaCl) at pH 7.2 (HEPES buffer). The fractions were used for western blot or ELISA to visualize the protein elution profiles.

Stromal Vascular Fraction (SVF) isolation

Stromal vascular cells were prepared from collagenase-digested adipose tissue and FACS analysis of stromal vascular cells for macrophage content and subtypes was performed as previously described (Li et al., 2010). The antibodies for surface staining were F4/80 (BM8), Ly6C (AL-21), CD11b (M1/70), and CD11c (N418) (eBioscience, San Diego, CA).

Statistics

Microarray results were normalized using RMA in the 'affy' package and differential expression p-values were calculated using the 'limma' package and adjusted for multiple comparisons by Benjamini-Hochberg procedure. All other data were analyzed by Student's *t* test or 2-way ANOVA and presented as mean ± SEM. Statistical analyses were performed using Prism software (version 5; GraphPad Software). *P* values less than 0.05 were considered significant.

Supplemental References

Bennett, B.J., Farber, C.R., Orozco, L., Kang, H.M., Ghazalpour, A., Siemers, N., Neubauer, M., Neuhaus, I., Yordanova, R., Guan, B., et al. (2010). A high-resolution association mapping panel for the dissection of complex traits in mice. Genome Res 20, 281-290.

Deng, Y., Foley, E.M., Gonzales, J.C., Gordts, P.L., Li, Y., and Esko, J.D. (2012). Shedding of syndecan-1 from human hepatocytes alters very low density lipoprotein clearance. Hepatology 55, 277-286.

Gonzales, J.C., Gordts, P.L., Foley, E.M., and Esko, J.D. (2013). Apolipoproteins E and AV mediate lipoprotein clearance by hepatic proteoglycans. J Clin Invest 123, 2742-2751.

Huang da, W., Sherman, B.T., and Lempicki, R.A. (2009a). Systematic and integrative analysis of large gene lists using DAVID bioinformatics resources. Nat Protoc 4, 44-57.

Huang da, W., Sherman, B.T., Zheng, X., Yang, J., Imamichi, T., Stephens, R., and Lempicki, R.A. (2009b). Extracting biological meaning from large gene lists with DAVID. Current protocols in bioinformatics / editoral board, Andreas D. Baxevanis ... [et al.] Chapter 13, Unit 13 11.

Khoo, J.C., Miller, E., Pio, F., Steinberg, D., and Witztum, J.L. (1992). Monoclonal antibodies against LDL further enhance macrophage uptake of LDL aggregates. Arteriosclerosis and thrombosis : a journal of vascular biology / American Heart Association 12, 1258-1266.

Lawrence, R., Olson, S.K., Steele, R.E., Wang, L., Warrior, R., Cummings, R.D., and Esko, J.D. (2008). Evolutionary differences in glycosaminoglycan fine structure detected by quantitative glycan reductive isotope labeling. J Biol Chem 283, 33674-33684.

Li, P., Lu, M., Nguyen, M.T., Bae, E.J., Chapman, J., Feng, D., Hawkins, M., Pessin, J.E., Sears, D.D., Nguyen, A.K., et al. (2010). Functional heterogeneity of CD11c-positive adipose tissue macrophages in diet-induced obese mice. J Biol Chem 285, 15333-15345.

Maccarana, M., and Lindahl, U. (1993). Mode of interaction between platelet factor 4 and heparin. Glycobiology 3, 271-277.

Nakaya, K., Tohyama, J., Naik, S.U., Tanigawa, H., MacPhee, C., Billheimer, J.T., and Rader, D.J. (2011). Peroxisome proliferator-activated receptor-alpha activation promotes macrophage reverse cholesterol transport through a liver X receptor-dependent pathway. Arterioscler Thromb Vasc Biol 31, 1276-1282.

Tacke, F., Alvarez, D., Kaplan, T.J., Jakubzick, C., Spanbroek, R., Llodra, J., Garin, A., Liu, J., Mack, M., van Rooijen, N., et al. (2007). Monocyte subsets differentially employ CCR2, CCR5, and CX3CR1 to accumulate within atherosclerotic plaques. J Clin Invest 117, 185-194.

Tacke, F., Ginhoux, F., Jakubzick, C., van Rooijen, N., Merad, M., and Randolph, G.J. (2006). Immature monocytes acquire antigens from other cells in the bone marrow and present them to T cells after maturing in the periphery. J Exp Med 203, 583-597.

Tsimikas, S., Miyanohara, A., Hartvigsen, K., Merki, E., Shaw, P.X., Chou, M.Y., Pattison, J., Torzewski, M., Sollors, J., Friedmann, T., et al. (2011). Human oxidation-specific antibodies reduce foam cell formation and atherosclerosis progression. J Am Coll Cardiol 58, 1715-1727.